

Common mechanism links spiral wave meandering and wave-front–obstacle separation

J. M. Starobin* and C. F. Starmer

*Departments of Medicine (Cardiology) and Computer Science, Duke University Medical Center,
P.O. Box 3181, Durham, North Carolina 27710*

(Received 6 May 1996; revised manuscript received 30 September 1996)

Spiral waves rotate either around a circular core or meander, inscribing a noncircular pattern. The medium properties determining the transition of meandering were found to be equivalent to those defining the transition from wave tip separation and attachment around the end of an unexcitable strip of thickness comparable to zero velocity wave-front thickness. The transition from circular to noncircular tip movement is analytically predicted by the balance of the diffusive fluxes within the boundary layer at the wave tip. [S1063-651X(97)11701-9]

PACS number(s): 47.32.Cc, 82.40.-g

Spiral waves appear in many excitable chemical and biological media [1]. The spiral wave tip either rotates around a circular unexcited core or meanders, inscribing a noncircular pattern often similar to that of a multipetal flower. From numerical studies of FitzHugh-Nagumo-like models for a variety of medium parameters, Zykov [2] and Winfree [3] found a distinct boundary separating meandering from circular tip movement, suggesting that transitions between different modes of tip movement were dependent on certain medium parameter values.

The transition from circular spiral tip motion to meandering is known to occur when the spiral tip approaches its refractory tail. The minimal distance between the spiral tip and refractory tail associated with the meandering transition and its relation to medium properties, though, is uncertain. Recently numerical studies of Karma [4] showed that meandering corresponds to the superposition of two rotating spiral wave solutions. He found that the reaction-diffusion field at points located on the wave front near the minimal core radius associated with the meandering transition (determined numerically) displayed quasiperiodic variations originating from a supercritical Hopf bifurcation. Analytical investigations of spiral core stability by Kessler *et al.* [5] based on kinematic theory did not confirm this behavior, probably because their analysis was performed within a kinematic framework that differed significantly from the framework of Karma's analysis [4]. Moreover, the kinematic approach is limited by the assumption that the wave radius of curvature is large compared with the wavelength, a condition that is not fulfilled at the spiral tip [6]. Barkley developed a phenomenological model that reproduced complex spiral tip movement [7]. However, based on the ordinary differential equation representation, this model did not describe the transition to meandering and did not provide a minimal core radius associated with a meandering transition boundary since it neglected generic diffusive properties of an excitable medium.

In this paper, we show that the conditions associated with the meandering transition are equivalent to conditions asso-

ciated with the transition between wave-front–obstacle attachment and separation following a wave-obstacle interaction [Fig. 1(a)]. We found that the minimal distance that the spiral wave tip can approach its refractory tail without meandering is of the order of L_{crit} , the wave-front thickness of a wave propagating with zero velocity. Following interaction with an unexcitable strip of thickness L_{crit} , there are two possible outcomes. If the wave tip wraps itself around the end of this unexcitable strip, then it will meander if the strip is removed. Alternatively, if the wave tip separates from the end of the strip, then removal will result in circular spiral tip motion. Over a range of medium parameters, this transition can be accurately predicted by approximating the diffusive fluxes within the boundary layer at the wave tip [9,10].

Here we consider nonlinear reaction-diffusion equations of the FitzHugh-Nagumo class:

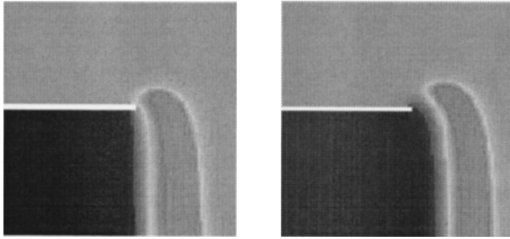
$$\frac{\partial u}{\partial t} = \frac{\partial^2 u}{\partial x^2} + \frac{\partial^2 u}{\partial y^2} + f(u) - V, \quad (1)$$

$$\frac{\partial V}{\partial t} = \varepsilon(\gamma u - V), \quad (2)$$

where $u(x,y,t)$ is a dimensionless function similar to the transmembrane potential in a biological excitable cell and $V(x,y,t)$ is a dimensionless function similar to a slower recovery current. Using this electrical analogy, we consider reaction-diffusion fluxes to be the flow of a charge (current) down a potential gradient. The nonlinear source of charge is determined by the function, $f(u)$, that represents the reactive properties of the medium. We consider $f(u)$ as a piecewise linear function similar to the current-voltage relationship of a nonlinear oscillator [Fig. 1(b)]. The slope of this function, λ , controls one aspect of excitability by determining the maximum current that is available to excite adjoining regions of the medium: larger values of λ result in a more excitable medium while smaller values of λ result in a less excitable medium. Excitability is also influenced by m_1 , m_2 , and m_3 , the zeros of $f(u)$ with respect to the equilibrium value of the recovery variable, V_{eq} . A highly excitable medium is determined by $m_2 - m_1 \ll m_3 - m_2$. The factors γ and ε (the

*Author to whom correspondence should be addressed. Fax: (919)684-8666. Electronic address: josephhodgkin.mc.duke.edu

A



B

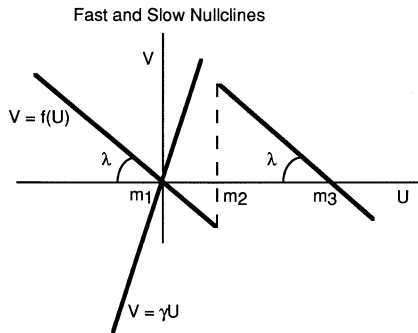


FIG. 1. (a) shows the computed temporal sequence (from left to right) of wave-front–obstacle interaction resulting in separation of the excitation wave from the unexcitable obstacle. The left frame demonstrates a fully formed spiral tip, which later separates from the strip (right frame). The width of the strip is of the order of the critical wave-front thickness shown in both fragments by a thin white line bounding the tip area. Computations were performed over a 170×170 grid using an implicit fractional-step method [8] with $\Delta x = \Delta y = 0.25$, $\Delta t = 0.2$. (b) shows the null-clines of the reaction diffusion system of Eqs. (1) and (2). We consider $u(x, y, t)$ as similar to the transmembrane potential of an excitable cardiac or nerve cell, $f(u)$ is similar to the current-voltage relationship of the cellular excitation process, and $V(x, y, t)$ is similar to slow recovery current. The function $f(u)$ is a piecewise linear function, where the slope of each linear element, λ , refers to the rate of the fast excitation process and influences medium excitability. The slope γ refers to the rate of the slow recovery process. For a 1D excitable cable and piecewise linear $f(u)$ the basic characteristics of wave propagation such as pulse propagation velocity, wave-front thickness, and the minimal wave-front thickness L_{crit} associated with a nonpropagating wave have been determined in [9,10].

ratio of fast to slow time constants), are relaxation parameters and $\varepsilon \ll 1$ [$\alpha = (m_3 - m_2)/(m_2 - m_1)$].

In order to explore the hypothesis that no separation from the obstacle is equivalent to meandering, we observed obstacle-wave interactions for a variety of model parameters, λ , α , and ε , in order to alter the wave-front charge while keeping the kinetics of recovery constant. We observed the transition from circular to noncircular tip movement as follows (Fig. 2): starting with a spiral rotating around a large core (left upper panel), as we increased the wave-front charge (by increasing λ), the spiral tip rotated about circular cores of progressively smaller radii (right upper panel) until the tip approached the refractory tail by a critical distance.

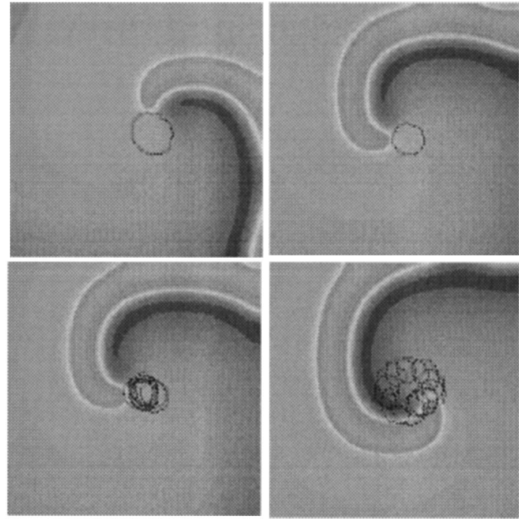


FIG. 2. Shown are four spirals of increasing wave-front charge as defined by the slope of the fast null-cline λ . Spiral waves were computed for $\varepsilon = 0.018$, $\alpha = 2.75$, and $\gamma = 7$ while varying λ and were initiated by a wave break created with the initial conditions. The spiral tip was tracked by following the path of the unstable point $u = m_2$, $V = V_{\text{eq}} = 0$. Upper panels (left, $\lambda = 0.86$ and right, $\lambda = 0.885$) show circular spiral tip movement. When $\lambda = 0.905$, the wave-front thickness is comparable to the core diameter and the tip begins to meander (low left panel). When λ is further increased to 0.93, meandering becomes very pronounced (low right panel).

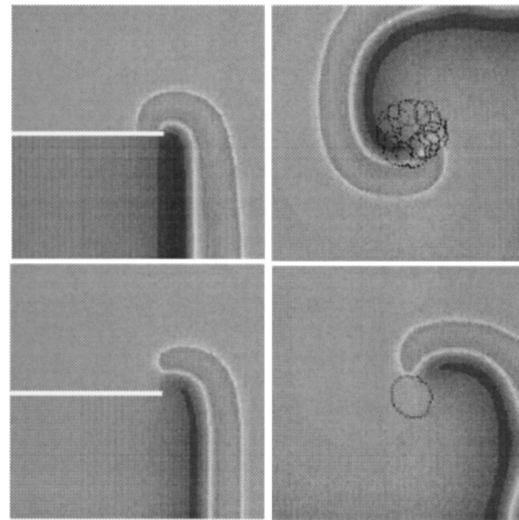


FIG. 3. Shown is the meandering transition coinciding with the wave-front–obstacle separation-attachment boundary. Spiral waves were computed for $\varepsilon = 0.018$, $\alpha = 2.75$, and $\gamma = 7$ while varying λ . Upper panels, $\lambda = 0.93$ (from left to right), demonstrate the excitation wave tip, which wraps around the unexcitable strip (left upper panel) approaching the refractory tail. This wave fragment meanders after obstacle removal (right upper panel). The width of the striplike obstacle (thin straight white line) is of the order of the wave-front thickness (white thin layer bounding the wave tip). As we decreased the wave-front charge by decreasing λ ($\lambda = 0.86$) the wave tip separated from the obstacle (lower left panel). This wave fragment rotated around a small unexcited circular core after obstacle removal (low right panel).

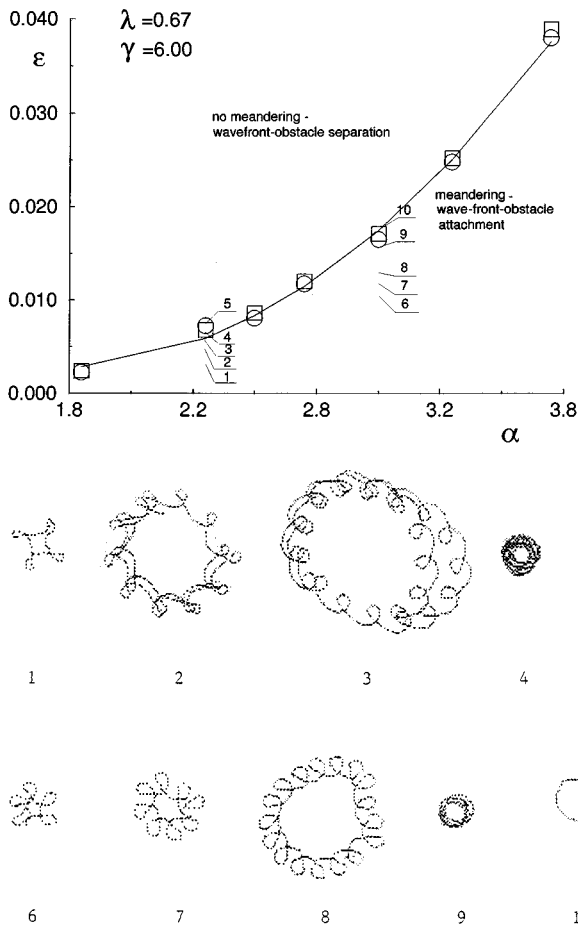


FIG. 4. The coincidence of the meandering transition with the wave-front–obstacle separation–attachment boundary (a) in the (ϵ, α) plane for $\lambda=0.67$ and $\gamma=6$. Squares illustrate the computed meandering transition while circles refer to a computed wave-front–obstacle separation–attachment boundary (solid line is a quadratic regression: $\epsilon = 0.028 - 0.03\alpha + 0.0087\alpha^2$). Computations were performed for the striplike unexcitable obstacles with the width that is of the order of the wave-front thickness [see Fig. 1(a)]. (b) illustrates the “flower garden” (tip trajectories) for points indicated in (a) by numbers 1,2,3,4,5 for $\alpha=2.3$; $\epsilon=0.032, 0.048, 0.057, 0.065, 0.075$ and numbers 6,7,8,9,10 for $\alpha=3.0$; $\epsilon=0.01, 0.0117, 0.0129, 0.0157, 0.0175$, respectively.

When the distance was less than this critical distance, the tip meandered (low panels left and right, respectively).

In our numerical experiments the critical distance between the spiral tip and a refractory tail associated with the meandering transition was always comparable to that of the zero velocity wave-front thickness, L_{crit} . Figure 3 demonstrates that if the tip approaches the refractory tail within a distance that is of the order of L_{crit} (thin white strip between the tip and the refractory tail), i.e., the tip is able to make a turn of diameter, L_{crit} , while maintaining attachment to the strip boundary (upper left panel) then meandering results after removal of the strip (upper right panel). Similarly, if the charge available in the wave front is insufficient to extend the tip around the corner of the strip (low left panel, lower excitability, λ) then the wave tip cannot approach the refractory tail sufficiently close. Consequently, the tip will rotate around a small circular unexcited core with a diameter

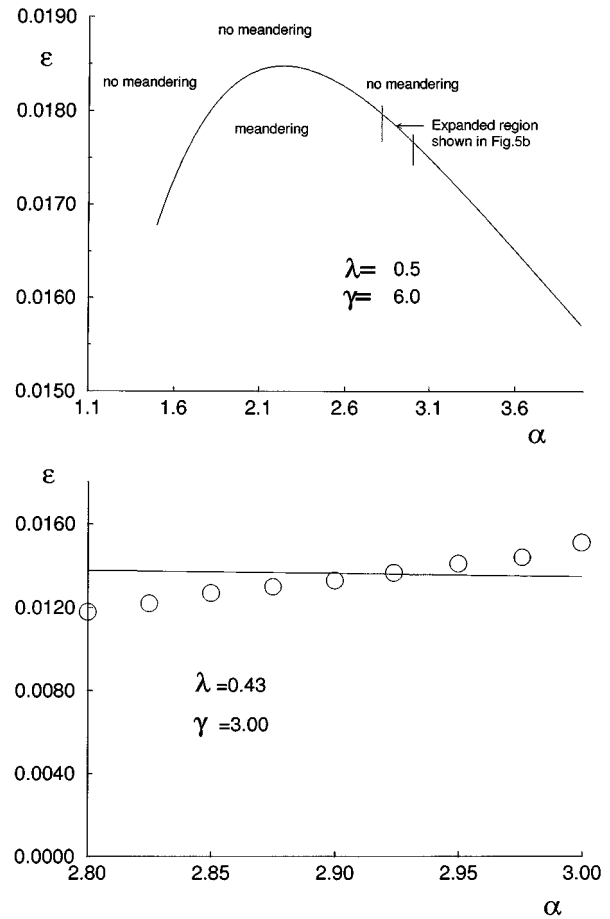


FIG. 5. The boundary defining the theoretical transitions between circular and noncircular tip motion. (a) illustrates qualitative agreement of Eq. (3) (in a wide range of α) with the multivalued meandering transition in the (ϵ, α) plane ($\gamma=6, \lambda=0.5$) as described in [2,6]. (b) illustrates quantitative agreement within the range of $\alpha=(2.8, 3.0)$. The solid line is the analytical estimation of the meandering transition boundary determined by Eq. (3) and the circles refer to numeric estimates.

$> L_{\text{crit}}$ after the strip is removed from the medium (low right panel).

Numerical studies demonstrated the equivalence between conditions for the wave-front–obstacle attachment–separation boundary and the boundary of the transition to meandering in the (ϵ, α) plane [Fig. 4(a)] over a wide range of medium parameters. Moreover, small changes in the parameter ϵ near the transition boundary resulted in a variety of flower configurations quite similar to those associated with the cubic $f(u)$ [2,3,7] as shown in Fig. 4(b).

The coincidence between the meandering transition and obstacle attachment–separation transition suggests a common mechanism for both transition processes, which is based on the balance of reaction–diffusion fluxes within a small boundary layer of the order of the zero velocity wave-front thickness, L_{crit} . Recently we showed that by discretizing this boundary layer with squares of the order of the zero velocity wave-front thickness, L_{crit} , it was possible to develop an analytical approximation of the separation–no separation boundary [10]. Whether the wave tip maintained the attachment or separated from the obstacle boundary depended on

what we called a charge balance C_B , derived from the integral form of the Eqs. (1) and (2) obtained by averaging them within a piecewise rectangular approximation of the boundary layer over the wave-front formation time. C_B was defined in terms of a relationship between the charge available within the wave front, the charge required to ignite the boundary layer, and the charge that leaks from the boundary layer into adjacent rested medium. When $C_B > 0$, wave-front-obstacle attachment was maintained while when $C_B < 0$, wave-front-obstacle separation occurred. For a striplike obstacle one can find the medium parameters associated with the wave-front-obstacle separation-attachment boundary from the equation $C_B = 0$, which is given by

$$\left[33 - \frac{47}{2\sigma^2} \frac{\alpha + 1}{\alpha - 1} \right] \lambda^3 + \frac{4(\alpha + 1)^3}{\alpha(\alpha - 1)} \lambda^2 - \varepsilon \frac{4\gamma(\alpha + 1)^5 \sigma}{\alpha^2(\alpha - 1)} = 0, \quad (3)$$

where $\sigma = 1 + \ln 2$, $\alpha = (m_3 - m_2)/(m_2 - m_1)$ [10]. Our numerical studies show that the same analysis can be applied to the transition between circular and noncircular tip motion. When $C_B < 0$, circular motion is expected. When $C_B > 0$ meandering is expected.

Equation (3) is in qualitative agreement with the multivalued meandering transition in the (ε, α) plane shown in [2,3,7] [Fig. 5(a)]. Comparison of numerical estimates of the meandering-no-meandering boundary and theoretical predictions of the wave-front-obstacle separation-attachment boundary [Eq. (3)] over a limited range of α reveals good quantitative agreement [Fig. 5(b)]. Numerical estimates outside this range are limited by the series approximation used in deriving Eq. (3) [10].

In summary, we determined the minimal distance between a spiral wave tip and its refractory tail associated with the meandering transition. We have found that if the wave tip approached its tail within a distance L_{crit} (wraps itself around

the end of an unexcitable strip of the order of the wave-front thickness), then it will meander if the strip is removed. Thus, we demonstrate that the transition from circular to noncircular spiral tip motion is determined by the same conditions for the transition from wave tip separation to attachment of the wave to the end of a thin (of the order of the zero velocity wave-front thickness) unexcitable strip and can be predicted from the medium properties by analysis of the boundary layer separating the spiral wave tip from the “virtual” obstacle [9,10].

Spiral core stability studies based on the analysis of temporal flux variations at fixed points (along the spiral core boundary) demonstrated unstable oscillating behavior at the spiral core [4,5]. However, these analyses yielded little insight about the medium conditions associated with the meandering transition and the minimal core radius (associated with meandering transition) which are determined by a full solution of the original partial differential equation reaction-diffusion system. By approximating the solution of the FitzHugh-Nagumo reaction-diffusion system Eqs. (1) and (2) in the region of the spiral tip, we have shown that the delicate balance between reaction-diffusion fluxes in this region and the surrounding boundary layer plays a major role in defining different types of spiral tip motion, thus affecting different instabilities of the spiral wave solution at points near the wave tip as described in [4,5]. Recognizing that small changes in the reaction-diffusion flux balance in the boundary layer can dramatically alter spiral tip motion provides a new tool for control of spiral wave processes and, in particular, control of cardiac arrhythmias.

We wish to acknowledge the critical assistance provided by V. N. Polotsky. His discussions were helpful in clarifying our results. This research was supported in part by Grant No. HL32994 from the National Heart, Lung, and Blood Institute, National Institutes of Health and a grant from the Whitaker Foundation.

- [1] A. T. Winfree, *When Time Breaks Down: The Three-Dimensional Dynamics of Electrochemical Waves and Cardiac Arrhythmias* (Princeton Univ. Press, Princeton, 1987).
 [2] V. S. Zykov, *Biofizika* **31**, 862 (1986).
 [3] A. T. Winfree, *Chaos* **1**, 303 (1991).
 [4] A. Karma, *Phys. Rev. Lett.* **65**, 2824 (1990).
 [5] D. A. Kessler, H. Levine, and W. Reynolds, *Phys. Rev. Lett.* **68**, 401 (1992); *Physica (Amsterdam)* **70D**, 115 (1994).
 [6] A. S. Mikhailov, *Foundations of Synergetics I. Distributed*

- Active Systems* (Springer, Berlin, 1990).
 [7] D. Barkley and I. G. Kevrekidis, *Chaos* **4**, 453 (1994).
 [8] R. D. Richtmayer, *Difference Methods for Initial-Value Problems* (Interscience, New York, 1957).
 [9] J. M. Starobin, Y. I. Zilberter, and C. F. Starmer, *Physica (Amsterdam)* **70D**, 321 (1994).
 [10] J. M. Starobin and C. F. Starmer, *Phys. Rev. E* **54**, 430 (1996); J. M. Starobin, Y. I. Zilberter, E. M. Rusnak, and C. F. Starmer, *Biophys. J* **70**, 581 (1996).